Differential Equations and Dynamical Systems (2020) 28:603–616
https://doi.org/10.1007/s12591-019-00502-x

ORIGINAL RESEARCH

Three-Dimensional Finite Element Model to Study Calcium Distribution in Astrocytes in Presence of VGCC and Excess Buffer

Brajesh Kumar Jha[1] · **Amrita Jha**[2] · **Neeru Adlakha**[3]

Published online: 13 November 2019

Abstract
The role of astrocytes in physiological processes is always a matter of interest for biologists, mathematicians and computer scientists. Similar to neurons, astrocytes propagate Ca^{2+} over long distances in response to stimulation and release gliotransmitters in a Ca^{2+}-dependent manner to modulate various important brain functions. There are various processes and parameters that affect the cytoplasmic calcium concentration level of astrocytes like calcium buffering, influx via calcium channels, etc. Buffers bind with calcium ion (Ca^{2+}) and makes calcium bound buffers. Thus, it decreases the calcium concentration [Ca^{2+}] level. Ca^{2+} enters into the cytosol through voltage gated calcium channel (VGCC) and thus it increases the concentration level. In view of above, a three-dimensional mathematical model is developed for combined study of the effect of buffer and VGCC on cytosolic calcium concentration in astrocytes. Finite element method is applied to find the solution using hexagonal elements. A computer programme is developed for entire problem to simulate the results. The obtained results show that high affinity buffer reveals the effect of VGCC and at low buffer concentration VGCC effects more significantly.

Keywords Ca^{2+} concentration · Buffer · Voltage gated calcium channel · Finite element method

Mathematics Subject Classification 65L60 · 62P10 · 92C35

✉ Brajesh Kumar Jha
brajeshjha2881@gmail.com

Amrita Jha
tripathi.amrita28@gmail.com

Neeru Adlakha
neeru.adlakha21@gmail.com

[1] Department of Mathematics, School of Technology, Pandit Deendayal Petroleum University, Raisan, Gandhinagar, Gujarat, India

[2] Department of Science and Humanities, Indus University, Ahmedabad, Gujarat, India

[3] Department of Applied Mathematics, S. V. National Institute of Technology, Surat, Gujarat, India

Introduction

Computational neuroscience has emerged as a new research area for mathematicians and theoretical scientists due to its complex physiology. One of the notable examples is modelling calcium signalling in glial cell like astrocytes. Astrocytes are found to be the most diverse population of glial cells in nervous system. Twenty years ago, the traditional view of astrocytes was merely as supportive cells providing only structural and metabolic support to neurons [1–3]. Recent studies of astrocytes have suggested that these cells not only supports the neurons but actively participates in the dynamic regulation of cerebral microcirculation, synaptic transmission and neuronal activation [2, 4–6]. Astrocytes are now widely accepted as nerve cells that propagate Ca^{2+} over long distances in response to stimulation and similar to neurons release transmitters (called gliotransmitters) in a Ca^{2+}-dependent manner [4, 7]. Spontaneous astrocytic Ca^{2+} oscillations have been observed and implicated in important functions of the brain. However, the mechanism of spontaneous Ca^{2+} oscillations is still unclear. Therefore, it is critical to understand how the Ca^{2+} oscillations are generated and modulated [7, 8].

There are so many processes involved in calcium signalling that effects the calcium concentration in cytosol. The notable examples are calcium buffering, entrance of calcium ion Ca^{2+} through voltage gated channels, etc. Mathematical problems have been formulated in the form of reaction–diffusion equation, advection diffusion equation for one- and two-dimensional cases. Tripathi et al. have studied the effect of several parameters like sodium calcium exchanger, buffer concentration, diffusion coefficients etc. on calcium concentration $[Ca^{2+}]$ in neuron [9–11]. Tewari et al. have developed the mathematical model to study the effect of sodium calcium exchanger, calcium buffering, VGCC etc. on calcium concentration in neuron for one- and two-dimensional cases [12, 13]. To find the solution, different numerical and analytical techniques have been used like Laplace transform, finite difference method (FDM), FEM, finite volume method (FVM), etc. FEM has gained general acceptance for handling the diversity of problems along with diverse geometrical configurations and boundary conditions which can be examined by a single computer programme. Jha et al. have developed two-dimensional reaction diffusion equation to study the effect of buffer concentration on cytosol in astrocytes [14]. Later on, the model is extended to study the comparative effect of buffer concentration and VGCC on cytosolic calcium concentration in astrocytes [15]. Naik et al. have studied the effect of RyR calcium channel, ER and SERCA pump on calcium distribution in Oocytes cell [16]. Before this, authors have studied the effect of various parameters in oocytes and T-lymphocyte using finite element method. In this paper we have extended the already present models [17–19] in three-dimensional mathematical model. The physiological results obtained are interpreted with neurological disorders like Alzheimer's and Parkinson's diseases using one and two dimensional mathematical models [20, 21]. In previous paper, study has been made for only point source. In this paper line source is incorporated to modulate more realistic situation. FEM is used to solve the problem. A computer program is developed for the entire problem to simulate the results.

Mathematical Formulation

Mathematical model is developed in the form of diffusion equation for steady state case. Calcium buffering and VGCC are included in the model. The formulation of calcium buffering and VGCC is given in subsequent subsections.

Calcium Buffering

Calcium buffers were examined for their ability to reduce evoked transmitter release when injected into the presynaptic terminal of the squid giant synapse. Ethylene glycol tetraacetic acid (EGTA) is virtually ineffective at reducing transmitter release, even at estimated intracellular concentrations. Conversely, the buffer 1,2-bis(*o*-aminophenoxy)ethane-*N*,*N*,*N*,*N*-tetraacetic acid (BAPTA) has an equilibrium affinity for calcium similar to that of EGTA, which produced a substantial reduction in transmitter release when injected in presynapse [22, 23]. Experimentally Wang et al. [23] first reported and illustrated directly that cytoplasmic calcium buffering constitutes an important and powerful mechanism for modulating astrocytic Ca^{2+} waves.

Calcium kinetics in astrocytes is governed by a set of reaction–diffusion equations which can be framed assuming the following bimolecular reaction between Ca^{2+} and buffer species [24, 25]

$$\left[Ca^{2+}\right] + \left[B_j\right] \underset{k_j^-}{\overset{k_j^+}{\Leftrightarrow}} \left[CaB_j\right] \tag{1}$$

where $[B_j]$ and $[CaB_j]$ are free and bound buffer respectively, and 'j' is an index over buffer species. The resulting partial differential equations in three dimensions for Eq. (1) using Fickian diffusion can be stated as [24, 26]

$$\frac{\partial\left[Ca^{2+}\right]}{\partial t} = D_{Ca}\left(\frac{\partial^2\left[Ca^{2+}\right]}{\partial x^2} + \frac{\partial^2\left[Ca^{2+}\right]}{\partial y^2} + \frac{\partial^2\left[Ca^{2+}\right]}{\partial z^2}\right) + \sum_j R_j + J_{VGCC} - P_{out}\left[Ca^{2+}\right] \tag{2}$$

$$\frac{\partial\left[B_j\right]}{\partial t} = D_{B_j}\left(\frac{\partial^2\left[B_j\right]}{\partial x^2} + \frac{\partial^2\left[B_j\right]}{\partial y^2} + \frac{\partial^2\left[B_j\right]}{\partial z^2}\right) + R_j \tag{3}$$

$$\frac{\partial\left[CaB_j\right]}{\partial t} = D_{CaB_j}\left(\frac{\partial^2\left[CaB_j\right]}{\partial x^2} + \frac{\partial^2\left[CaB_j\right]}{\partial y^2} + \frac{\partial^2\left[CaB_j\right]}{\partial z^2}\right) - R_j \tag{4}$$

where

$$R_j = -k_j^+[B_j][Ca^{2+}] + k_j^-[CaB_j] \tag{5}$$

D_{Ca}, D_{B_j}, D_{CaB_j} are diffusion coefficients of free calcium, free buffer and Ca^{2+} bound buffer respectively. k_j^+ and k_j^- are association and dissociation rate constants for buffer 'j' respectively.

Voltage Gated (Operated) Calcium Channel

Astrocytes were shown to express voltage-gated $[Ca^{2+}]$ channels similar to those found in neurons [1, 27]. Later, it was found that Ca^{2+} influx through voltage-gated ion-channels significantly increases cytosolic calcium concentration $[Ca^{2+}]_i$ in astrocytes. Voltage-gated Ca^{2+} channels form an important path way for $[Ca^{2+}]$ entry in excitable cells; the later

have been found to express a variety of $[Ca^{2+}]$ channels, differing in their voltage dependence, kinetics, and pharmacological properties [28, 29]. Calcium channels are integral membrane proteins composed of five subunits, each playing a distinct role in channel function. MacVicar first demonstrated Ca^{2+} action potentials in cAMP-treated cultured cortical astrocytes when the K^+ conductance was blocked and 10 mM Ba^{2+} was added [30]. The Ca^{2+} current has been modelled using the Goldman–Hodgkin–Katz (GHK) current equation as given below [26, 30].

$$I_{Ca} = P_{Ca} z_{Ca}^2 \frac{F^2 V_m}{RT} \frac{[Ca]_i - [Ca]_0 \exp\left(-z_{Ca} \frac{FV_m}{RT}\right)}{1 - \exp\left(-z_{Ca} \frac{FV_m}{RT}\right)} \tag{6}$$

where $\left[Ca^{2+}\right]_i$ and $\left[Ca^{2+}\right]_0$, are the intracellular and extracellular calcium concentrations respectively. P_{Ca} is the permeability of calcium ion, z_{Ca} is the valency of calcium ion. F is Faraday's constant. V_m is membrane potential. R is Real gas constant and T is Absolute temperature. Equation (6) is converted into molar/second by using the following equation

$$\sigma_{Ca} = \frac{-I_{Ca}}{z_{Ca} F V_{Ast}} \tag{7}$$

The negative sign in Eq. (7) is taken because, by convention the inward current is taken to be negative. GHK current equation gives the current density as a function of voltage. The GHK equation is derived from the constant field which assumes that the electric field in the membrane is constant and thus ions move in the membrane as in free solution.

For stationary immobile buffers of fixed buffers $D_{B_j} = D_{CaB_j} = 0$. Further Eqs. (2–7) can be written for steady state as

$$\begin{aligned} &D_{Ca}\left(\frac{\partial^2\left[Ca^{2+}\right]}{\partial x^2} + \frac{\partial^2\left[Ca^{2+}\right]}{\partial y^2} + \frac{\partial^2\left[Ca^{2+}\right]}{\partial z^2}\right) - k_j^+ [B]_\infty \left(\left[Ca^{2+}\right] - \left[Ca^{2+}\right]_\infty\right) \\ &+ \frac{P_{Ca} z_{Ca} F V_m}{RT V_{Ast}} \frac{[Ca]_i - [Ca]_0 \exp\left(-z_{Ca} \frac{FV_m}{RT}\right)}{1 - \exp\left(-z_{Ca} \frac{FV_m}{RT}\right)} - P_{out}\left[Ca^{2+}\right] + \sigma_{Ca} = 0 \end{aligned} \tag{8}$$

Considering the point source of calcium at. Thus the VGCC at boundary condition can be given as

$$\left.\begin{aligned} -D_{Ca} \frac{d\left[Ca^{2+}\right]}{dx} &= \sigma_{Ca}, \quad x = 0\ ,\ 0 \le y \le 5,\ 0 \le z \le 5. \\ -D_{Ca} \frac{d\left[Ca^{2+}\right]}{dy} &= \sigma_{Ca}, \quad y = 0\ ,\ 0 \le x \le 5,\ 0 \le z \le 5. \\ -D_{Ca} \frac{d\left[Ca^{2+}\right]}{dz} &= \sigma_{Ca}, \quad z = 0\ ,\ 0 \le x \le 5,\ 0 \le y \le 5. \end{aligned}\right\} \quad x = y = z = 0 \tag{9}$$

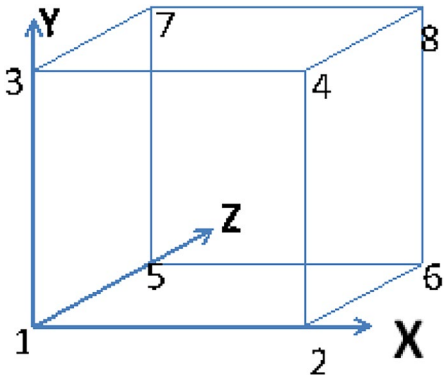

Fig. 1 Descretization of the domain in three dimensions

Also, the background concentration of $[Ca^{2+}]$ is 0.1 μM. As moving far away from the source. The calcium concentration

$$\left[Ca^{2+}\right] = 0.1\,\mu M \quad at \quad x = y = z = 5 \tag{10}$$

For the convenience the Eq. (8) can be written as

$$\frac{\partial^2 u}{\partial x^2} + \frac{\partial^2 u}{\partial y^2} + \frac{\partial^2 u}{\partial z^2} - au + b = 0 \tag{11}$$

The discretized variational form of Eq. (11) can be written as:

$$I^{(e)} = \frac{1}{2}\iiint_{\Omega}\left\{\left(\frac{\partial u^{(e)}}{\partial x}\right)^2 + \left(\frac{\partial u^{(e)}}{\partial y}\right)^2 + \left(\frac{\partial u^{(e)}}{\partial z}\right)^2 + au^{(e)^2} - 2bu^{(e)}\right\}dxdydz - \mu^{(e)}\int_{x_i}^{x_j}\left(\frac{\sigma}{D_{Ca}}u^{(e)}\Big|_{x=5}\right)dy \tag{12}$$

Here, we have used 'u' in lieu of $[Ca^{2+}]$ for our convenience, e = 1 2…125. In the term outside the integral, $\mu^{(e)} = 1$ for e = 1 and $\mu^{(e)} = 0$ for rest of the elements. The shape function of concentration variation within each element is defined by [31] and shown in Fig. 1.

$$u^{(e)} = c_1^{(e)} + c_2^{(e)}x + c_3^{(e)}y + c_4^{(e)}z + c_5^{(e)}xy + c_6^{(e)}yz + c_7^{(e)}zx + c_8^{(e)}xyz \tag{13}$$

$$u^{(e)} = P^T c^{(e)} \tag{14}$$

where, $P^T = \left[\,1 \;\; x \;\; y \;\; z \;\; xy \;\; yz \;\; zx \;\; xyz\right]$ and

$$c^{(e)^T} = \left[\; c_1^{(e)} \;\; c_2^{(e)} \;\; c_3^{(e)} \;\; c_4^{(e)} \;\; c_5^{(e)} \;\; c_6^{(e)} \;\; c_7^{(e)} \;\; c_8^{(e)} \;\right] \tag{15}$$

From Eq. (14) and (15) we get

$$\bar{u}^{(e)} = P^{(e)}c^{(e)} \tag{16}$$

where $\bar{u}^{(e)} = \begin{bmatrix} u_i \\ u_j \\ u_k \\ u_l \\ u_{i'} \\ u_{j'} \\ u_{k'} \\ u_{l'} \end{bmatrix}$ and $P^{(e)} = \begin{bmatrix} 1 & x_i & y_i & z_i & x_iy_i & y_iz_i & z_ix_i & x_iy_iz_i \\ 1 & x_j & y_j & z_j & x_jy_j & y_jz_j & z_jx_j & x_jy_jz_j \\ 1 & x_k & y_k & z_k & x_ky_k & y_kz_k & z_kx_k & x_ky_kz_k \\ 1 & x_l & y_l & z_l & x_ly_l & y_lz_l & z_lx_l & x_ly_lz_l \\ 1 & x_{i'} & y_{i'} & z_{i'} & x_{i'}y_{i'} & y_{i'}z_{i'} & z_{i'}x_{i'} & x_{i'}y_{i'}z_{i'} \\ 1 & x_{j'} & y_{j'} & z_{j'} & x_{j'}y_{j'} & y_{j'}z_{j'} & z_{j'}x_{j'} & x_{j'}y_{j'}z_{j'} \\ 1 & x_{k'} & y_{k'} & z_{k'} & x_{k'}y_{k'} & y_{k'}z_{k'} & z_{k'}x_{k'} & x_{k'}y_{k'}z_{k'} \\ 1 & x_{l'} & y_{l'} & z_{l'} & x_{l'}y_{l'} & y_{l'}z_{l'} & z_{l'}x_{l'} & x_{l'}y_{l'}z_{l'} \end{bmatrix}$

From the Eq. (14) we have

$$c^{(e)} = R^{(e)}\bar{u}^{(e)} \tag{17}$$

where

$$R^{(e)} = P^{(e)^{-1}} \tag{18}$$

Substituting $c^{(e)}$ from Eqs. (14), (16) and (17) we get

$$u^{(e)} = P^T R^{(e)}\bar{u}^{(e)} \tag{19}$$

Now the integral $I^{(e)}$ can be written in the form

$$I^{(e)} = I_k^{(e)} + I_m^{(e)} - I_s^{(e)} - I_z^{(e)} \tag{20}$$

where

$$I_k^{(e)} = \frac{1}{2}\iiint_{\Omega}\left\{\left(\frac{\partial u^{(e)}}{\partial x}\right)^2 + \left(\frac{\partial u^{(e)}}{\partial y}\right)^2 + \left(\frac{\partial u^{(e)}}{\partial z}\right)^2\right\}dxdydz \tag{21}$$

$$I_m^{(e)} = \frac{1}{2}\iiint_{\Omega}\frac{u^{(e)^2}}{\lambda^2}\,dxdydz \tag{22}$$

$$I_s^{(e)} = \frac{1}{2}\iiint_{\Omega}\left\{\frac{2u^{(e)}u_\infty}{\lambda^2}\right\}dxdydz \tag{23}$$

$$I_z^{(e)} = \frac{1}{2}\mu^{(e)}\int_{x_i}^{x_j}\left(\frac{\sigma}{D_{Ca}}u^{(e)}\Big|_{x=5}\right)dy \tag{24}$$

Now we extremize I w.r.t. each nodal calcium concentration u_i as given below

$$\frac{dI}{d\bar{u}} = \sum_{e=1}^{N}\bar{M}^{(e)}\frac{dI^{(e)}}{d\bar{u}^{(e)}}\bar{M}^{(e)T} = 0 \tag{25}$$

where, $\bar{M}^{(e)} = \begin{bmatrix} & 1\ 0\ 0\ 0 & & & 0\ 0\ 0\ 0 & \\ & 0\ 1\ 0\ 0 & & & 0\ 0\ 0\ 0 & \\ & 0\ 0\ 0\ 0 & & & 0\ 0\ 0\ 0 & \\ & \cdot\ \cdot\ \cdot\ \cdot & & & \cdot\ \cdot\ \cdot\ \cdot & \\ 0 & 0\ 0\ 0 & 0 & 0 & 0\ 0\ 0 & 0 \\ 0 & 0\ 0\ 1 & 0 & 0 & 0\ 0\ 0 & 0 \\ 0 & 0\ 0\ 0 & 1 & 0 & 0\ 0\ 0 & 0 \\ \cdot & \cdot\ \cdot\ \cdot & \cdot & \cdot & \cdot\ \cdot\ \cdot & \cdot \\ 0 & 0\ 0\ 0 & 0 & 1 & 0\ 0\ 0 & 0 \\ 0 & 0\ 0\ 0 & 0 & 0 & 1\ 0\ 0 & 0 \\ 0 & 0\ 0\ 0 & 0 & 0 & 0\ 0\ 0 & 0 \\ 0 & 0\ 0\ 0 & 0 & 0 & 0\ 0\ 1 & 0 \\ 0 & 0\ 0\ 0 & 0 & 0 & 0\ 0\ 0 & 1 \end{bmatrix}$ and

$I = \sum_{e=1}^{125} I^{(e)} \qquad \bar{u} = \begin{bmatrix} u_1 \\ u_2 \\ \vdots \\ \vdots \\ \vdots \\ \vdots \\ \vdots \\ u_{216} \end{bmatrix}$

$$\frac{dI^{(e)}}{d\bar{u}^{(e)}} = \frac{dI_k^{(e)}}{d\bar{u}^{(e)}} + \frac{dI_m^{(e)}}{d\bar{u}^{(e)}} - \frac{dI_s^{(e)}}{d\bar{u}^{(e)}} - \frac{dI_p^{(e)}}{d\bar{u}^{(e)}} \tag{26}$$

This leads to a following system of linear algebraic equations.

$$[K]_{216\times 216}[\bar{u}]_{216\times 1} = [F]_{216\times 1} \tag{27}$$

Here $\bar{u} = u_1, u_2, \ldots u_{216}$, K is the system matrices, and F is system vector. The Gaussian elimination method is employed to solve the system (27).

Results and Discussion

The numerical results for calcium profile against different biophysical parameters have been obtained using numerical values of parameter given in Table 1 unless stated along with the figures.

Table 1 Values of physiological parameters of astrocytes [15, 17, 24]

Symbol	Parameter	Value
D_{Ca}	Diffusion coefficient	250 $\mu m^2/s$
σ	Source amplitude	1pA
V_{ast}	Volume of the cytosol	$5.233 \times 10^{-13} l$
F	Faraday's constant	96,485 Coul/mole
R	Ideal gas constant	8.31 J/(mole K)
T	Temperature	300 K
P_{out}	Rate of calcium efflux from the cytosol	0.5 s^{-1}
Z_{Ca}	Valance of Ca^{2+} ion	2

Figure 2 shows the variation of $[Ca^{2+}]$ along the distance in x-axis. Cytosolic $[Ca^{2+}]$ profile moves from high concentration to low concentration so it is highest at the source and it decrease rapidly up to 2 μm and after that it attains its background concentration of 0.1 μM as it goes far away from the source. The combined effect of buffer and VGCC has been shown in Fig. 2. The obtained result is in agreement with the previous results obtained in literature [14–16]. For the comparative study, the graph is plotted below to show the effect of low and high amount of buffer concentration and VGCC along x, y, and z directions.

In Fig. 3, the spatial variation in calcium profile is shown in two-dimensional way considering (a) x and y (b) x and z and (c) y and z directions. Calcium concentration is higher at the mouth of the channel and it decrease rapidly up to 2 μm far from the source and then attains the background concentration. Since space is taken cubical and the flow of ion is considered smooth, the movement of calcium profile is found same in all x, y, and z directions. The behaviour of calcium profile is same as that of shown in Fig. 2. Since buffers exist near the plasma membrane of the cell, most of the free calcium ions are bonded by the buffers and makes calcium bound buffer near the source. Due to calcium buffering nerve cells control the flow of transmitters from one cell to another cell or synapse. Also this mechanism saves the nerve cell from the toxicity rendered due to high amount of calcium.

Figure 4a, b shows the variation in calcium profile along x and y directions. Calcium concentration decrease rapidly up to $x = 2$ μm (Fig. 4a) and $x = 1$ μm (Fig. 4b) then maintain the background concentration of 0.1 μM as move far away from the source. This difference is due to the presence and low of VGCC. Due to presence of voltage gated calcium channel more free calcium ion remains present in cytosol, so that concentration remains high near the source. Due to high free calcium concentration level, neurotransmitter (in glial cell like astrocytes) moves from one cell to another or in synapse in vesicular way. Both the buffers and the voltage gated calcium channels play important role in signalling

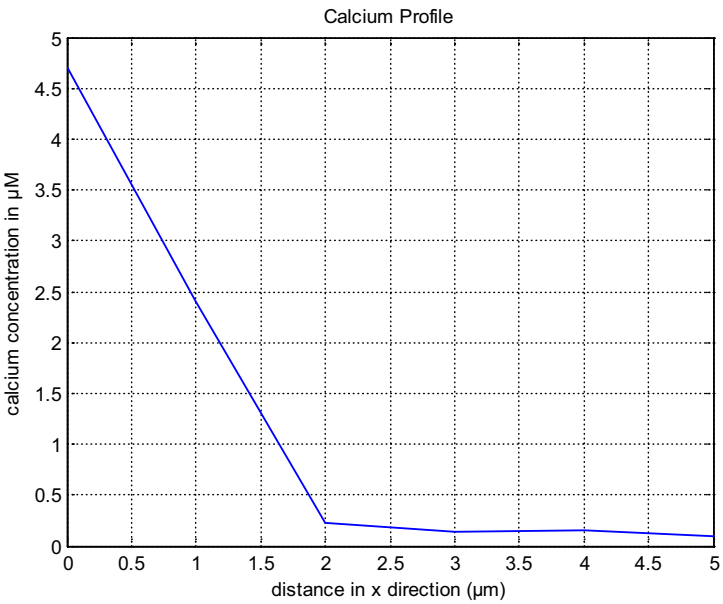

Fig. 2 Calcium distribution along x direction with buffer and VGCC

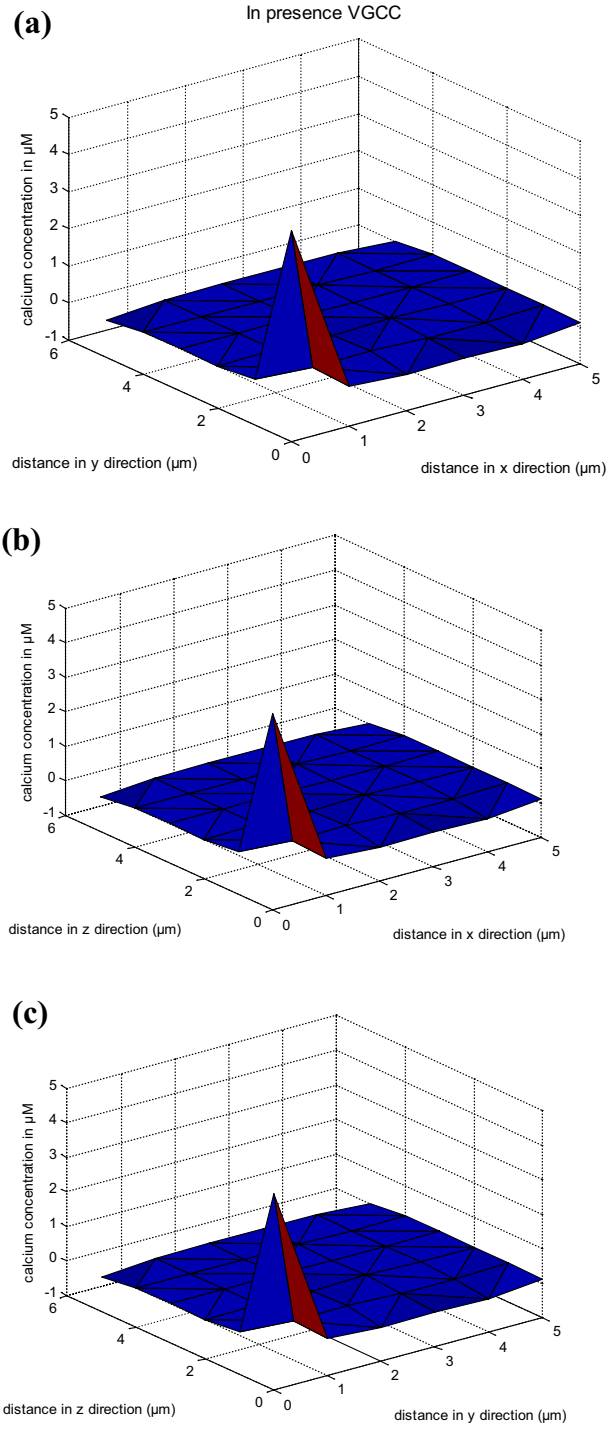

Fig. 3 Spatial variation of calcium concentration in **a** x and **b** y and x and z and **c** y and z direction in presence of buffers and VGCC

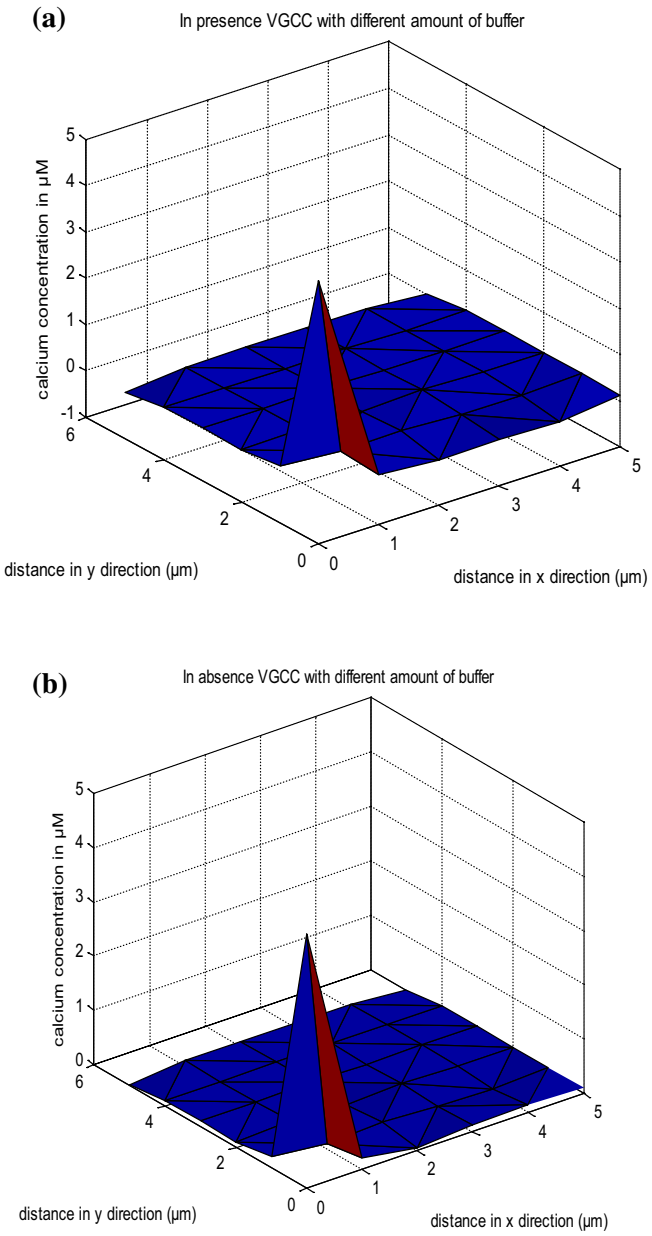

Fig. 4 **a**, **b** Calcium Concentration at different distance from point source along x and y direction for B = 30 μM k^{+}=1.5 μM/s, D_{Ca} = 250 μM^2/s in presence and low of VGCC

process of nervous system. Thus from Fig. 4a, b it is observed that the voltage gated calcium channel affect the calcium concentration level significantly in astrocytes.

Figure 5 shows the calcium profile along two direction namely x and y axis in (a) presence and (b) low of VGCC. The line source is considered at the boundary. It is

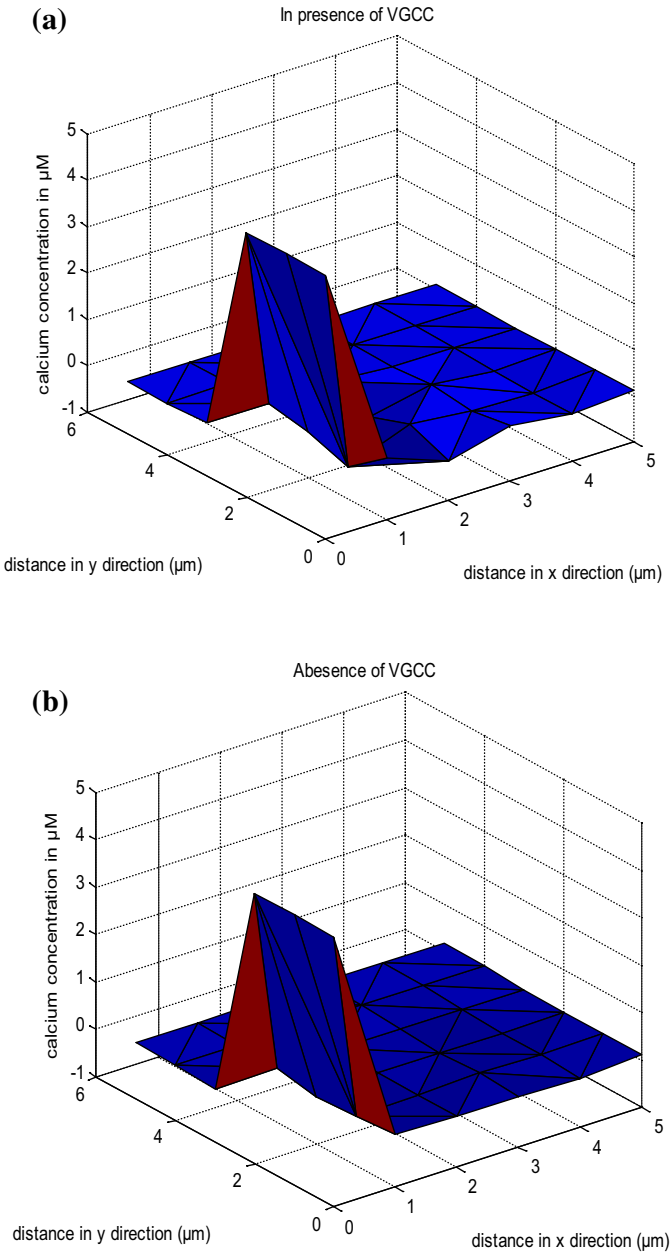

Fig. 5 **a**, **b** Calcium concentration at different distance from line source along x and y direction for B = 30 μM k^{+}=1.5 μM/s, D_{Ca} = 250 μM^2/s in presence and low of VGCC

assumed that more channels are nearer to each other and makes line source. Calcium concentration decrease rapidly near the source and maintain the background concentration as it moves far away from the source. In low of VGCC (Fig. 5b) calcium profile decrease more sharply than the presence of VGCC (Fig. 5a). Thus, both the buffers and

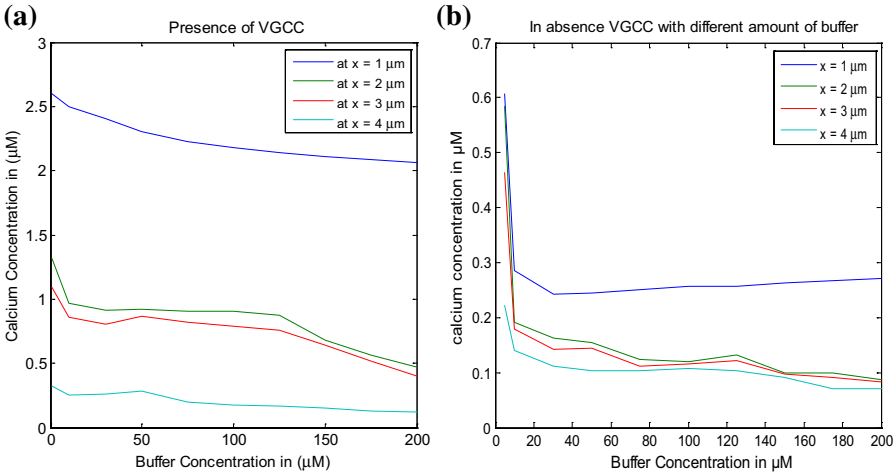

Fig. 6 **a**, **b** Calcium concentration at different distance from source, B = 5–200 μM, k^{+}=1.5 μM/s, D_{Ca} = 250 μM^2/s in presence and low of VGCC

voltage gated calcium channel plays their important role in calcium distribution in nerve cells like astrocytes.

Figure 6a shows the variation of [Ca^{2+}] along the x-axis for different amount of buffer at different position (x = 1, 2, 3, 4 μm) in cytosol in presence of different amount of buffer concentration B = 0–100 μ M and in presence of VGCC. As with the increase in the buffer concentration it is observed that with increase in buffer concentration, the calcium concentration decreases at x = 1 μm, 2 μm. Figure 6b shows the variation of [Ca^{2+}] along the x-axis for different amount of buffer at different positions (x = 1, 2, 3, 4 μm) in cytosol due to different values of buffer concentration B = 0–100 μ M in low of VGCC. We observe significant difference in concentration profiles in astrocytes from Fig. 6a in the presence of VGCC. It happens due to presence and low of VGCC.

Conclusion

The three-dimensional finite element model has been developed for a steady state case to study effect of buffer EGTA and VGCC, and influx on calcium concentration distribution in astrocytes. The dimension of the model is extended from two dimensions to three dimensions. The finite element method is quite flexible and versatile in the present situation as it has been possible to incorporate the parameters like EGTA, VGCC, influx and diffusion coefficient in the model. The results indicate that EGTA and VGCC has significant effect on calcium profile in the astrocytes. Also, the influx has significant effect on calcium distribution in astrocytes. Further, it can be concluded that VGCC plays more important role in calcium regulation in the low amount of buffers. The buffers are completely saturated and do not have the capacity to bind or in case of failure of buffers to bind calcium due to any abnormality or damage caused to buffers, etc. As any alteration in calcium distribution

in nerve cells are directly related neurological disorders like Alzheimer's and Parkinson's diseases. Such models can be developed further to study the relationship among various parameters under normal and abnormal conditions to generate information which can be of great use to biomedical scientists for clinical applications in neuronal diseases.

References

1. Deitmer, J.W., Verkhratsky, A.J., Lohr, C.: Calcium signalling in glial cells. Cell Calcium **24**, 405–416 (1998)
2. Verkhratsky, A., Butt, A.: Glial Neurobiology: A Textbook. Wiley, New York (2007)
3. Fellin, T.: Communication between neuron and astrocytes: relevance to the modulation of synaptic and network activity. J. Neurochem. **108**(3), 533–544 (2009)
4. Nedergaard, M., Rodriguez, J.J., Verkhratsky, A.: Glial calcium and disease of the nervous system. Cell Calcium **47**, 140–149 (2010)
5. Liu, Q.S., Xu, Q., Kang, J., Nedergaard, M.: Astrocyte activation of presynaptic metabotropic glutamate receptors modulates hippocampal inhibitory synaptic transmission. Neuron Glia Biol. **1**, 307–316 (2004)
6. Fiacco, T.A., Agulhon, C., McCarthy, K.D.: Sorting out astrocyte physiology from pharmacology. Annu. Rev. Pharmacol. Toxicol. **49**, 151–174 (2009)
7. Cornell-Bell, A., Finkbeiner, S.M.: Ca^{2+} waves in astrocytes. Cell Calcium **12**, 185–204 (1991)
8. Zeng, S., Li, B., Zeng, S., Chen, S.: Simulation of spontaneous Ca^{2+} oscillations in astrocytes mediated by voltage-gated calcium channels. Biophys. J. **97**, 2429–2437 (2009)
9. Jha, A., Adlakha, N., Jha, B.: Finite element model to study effect of Na^{+}–Ca^{2+} exchangers and source geometry on calcium dynamics in a neuron cell. J. Mech. Med. Biol. **16**(2), 1–22 (2015)
10. Jha, A., Adlakha, N.: Finite element model to study the effect of exogenous buffer on calcium dynamics in dendritic spines. Int. J. Model. Simul. Sci. Comput. **5**(2), 1–12 (2014)
11. Jha, A., Adlakha, N.: Analytical solution of two dimensional unsteady state problem of calcium diffusion in a neuron cell. J. Med. Imaging Health Inform. **4**(4), 547–553 (2014)
12. Tewari, S.G., Pardasani, K.R.: Modeling effect of sodium pump on calcium oscillations in neuron cells. J. Multiscale Model. **4**(3), 1–16 (2012)
13. Tewari, S.G., Pardasani, K.R.: Finite element model to study two dimensional unsteady state cytosolic calcium diffusion in presence of excess buffers. IAENG Int. J. Appl. Math. **40**(3), 108–112 (2010)
14. Jha, B.K., Adlakha, N., Mehta, M.N.: Two-dimensional finite element model to study calcium distribution in astrocytes in presence of excess buffer. Int. J. Biomath. **7**(3), 1–11 (2014)
15. Jha, B.K., Adlakha, N., Mehta, M.: Two-dimensional finite element model to study calcium distribution in astrocytes in presence of VGCC and excess buffer. Int. J. Model. Simul. Sci. Comput. **4**(2), 1250030-1–1250030-15 (2016)
16. Naik, P.A., Pardasani, K.: Finite element model to study calcium distribution in oocytes involving voltage gated calcium channel, ryanodine receptor and buffers. Alex. J. Med. **52**(1), 43–49 (2016)
17. Naik, P.A., Pardasani, K.: 2D finite element analysis of calcium distribution in oocytes. Netw. Model. Anal. Health Inform. Bioinform. **7**, 1–11 (2018)
18. Kumar, H., Naik, P.A., Pardasani, K.: Finite element model to study calcium distribution in T lymphocyte involving buffers and ryanodine receptors. Proc. Natl. Acad. Sci. India Sect. A **88**(4), 585–590 (2018)
19. Naik, P.A., Pardasani, K.: Three dimensional finite element model to study effect of RyR calcium channel, ER leak and SERCA pump on calcium distribution in oocyte cell. Int. J. Comput. Methods **16**(1), 1–19 (2019)
20. Dave, D.D., Jha, B.K.: Analytically depicting the calcium diffusion for Alzheimer's affected cell. Int. J. Biomath. **11**(7), 1–17 (2018)
21. Jha, B.K., Joshi, H., Dave, D.D.: Portraying the effect of calcium-binding proteins on cytosolic calcium concentration distribution fractionally in nerve cells. Interdiscip. Sci. Comput. Life Sci. **10**(4), 674–685 (2018)
22. Adler, E., Augustine, G., Duffy, S., Charlton, M.: Alien intracellular calcium chelators attenuate neurotransmitter release at the squid giant synapse. J. Neurosci. **11**(6), 1496–1507 (1991)

23. Wang, Z., Tymianski, M., Jones, O.T., Nedergaard, M.: Impact of calcium buffering on the spatial and temporal characteristics of intercellular calcium signals in astrocytes. J. Neurosc. **17**(19), 7359–7371 (1997)
24. Smith, G.D., Dai, L., Miura, R.M., Sherman, A.: Asymptotic analysis of buffered calcium diffusion near a point source. SIAM J. Appl. Math. **61**, 1816–1838 (2000)
25. Smith, G.D.: Analytical steady-state solution to the rapid buffering approximation near an open Ca^{2+} channel. Biophys. J. **71**, 3064–3072 (1996)
26. Keener, J., Sneyd, J.: Mathematical physiology, vol. 8, pp. 53–56. Springer, Berlin (1998)
27. Verkhratsky, A., Rodríguez, J.J., Parpura, V.: Molecular and cellular endocrinology calcium signalling in astroglia. Mol. Cell. Endocrinol. **353**(1–2), 45–56 (2012)
28. Hofmann, F., Biel, M., Flockerzi, V.: Molecular basis for Ca^{2+} channel diversity. Annu. Rev. Neurosci. **17**, 399–418 (1994)
29. Huguenard, J.R.: Low threshold calcium currents in central nervous system. Annu. Rev. Physiol. **58**, 329–348 (1996)
30. Macvicar, B.A.: Voltage-dependent calcium channels in glial cells. Science **226**, 1345–1347 (1984)
31. Rao, S.S.: Finite element method in engineering. Books. Elsevier Science and Technology, New York (2004)